Frontiers in Cancer Research (2021) Volume 1 Issue 1, *pp.* 1–10.
doi: 10.24294/fcr.v1i1.****

ORIGINAL RESEARCH ARTICLE

Synthesis of gold nanoparticles and its application in mercury ion etection

Baodui Wang 1,*, Tianrong Li 1, Jun Hai 1, Yongmin Liang 1, 2, Zhengyin Yang 2

[1] Catalysis, Indian Institute of Chemical Technology, Hyderabad·500007, India. E • mail: kannapuhari@gmail.com

[2] Department of Chemical Engineering, Hanyang University, Seoul 133·791, Republic of Korea. E •mail: ywsuh@hanyang.ac.kr

[3] Research Institute of Industrial Science, Hanyang University, Seoul 133·791, Republic of Korea. E • mail: hari83@hany ang.ac.kr wangbd@lzu.edu.cn

ABSTRACT

Gold nanoparticles (Au NPs) were synthesized by reducing $HAuCl_4$ with sodium citrate. The sensitivity and selectivity of gold amalgam The sensitivity and selectivity of gold amalgam catalytic degradation of rhodamine B(RhB) system for mercury detection were investigated by fluorescence spectroscopy and ultraviolet·visible In the experiment, students' interest in scientific research and exploratory spirit will be stimulated, In the experiment, students' interest in scientific research and exploratory spirit will be stimulated, students' comprehensive experimental operation skills and subjective initiative will be improved, the understanding and application The understanding and application of nanoparticles preparation, characterization, catalytic reaction knowledge and metal ion analysis methods will be enhanced. Further, the innovative thinking and scientific spirit of the students will be cultivated.

Keywords: Au nanoparticles; Rhodamine B; Hg^{2+}; Detection

1. Overview

With the development of nano and nanotechnology, the use of nanoprobes to detect heavy metal ions in water has attracted increasing research interest [1, 2], however, the use of nanoprobes to detect heavy metal ions in water is basically absent in undergraduate comprehensive analytical chemistry experiments. Most of the traditional analytical chemistry experiments are repetitive and outdated, and it is difficult to transfer the latest knowledge to students, thus largely limiting their analytical and problem·solving abilities and innovative awareness. The experimental teaching of nano·probe detection of heavy metal ions in water can not only enrich the basic knowledge of undergraduates, but also enable students to better adapt to the development of modern science and technology, therefore, the development of such experiments is of great significance.

ARTICLE INFO
Received: July 7, 2021 | Accepted: July 7, 2021 | Available online: August 7, 2021

CITATION
Prasad H, Suh YW, Vaddeboina V. Nano CoO-Cu-MgO catalyst for vapor phase simultaneous synthesis of ortho-chloroaniline and γ-butyrolactone from or-thocholonitrobenzne and 1,4-butanediol. Frontiers in Cancer Research 2021; 1(1): xxx.

The physical and chemical properties of gold nanoparticles (Au NPs) are related to their size,

shape and degree of aggregation [3]. Based on the properties of AuNPs, bioanalytical assays with high selectivity and sensitivity can be developed, and Au NPs can be used in a wide range of bioanalytical and biomedical detection techniques [4, 5]. The analytical methods using Au NPs as probes usually have the advantages of simplicity, rapidity and high sensitivity, and can be applied to actual sample detection. Mercury is a highly toxic heavy metal element, and the divalent form of mercury ion (Hg^{2+}) is the most common and stable form of mercury contamination [6]. Among the reported assays for Hg^{2+}, the colorimetric method has received much attention due to its outstanding advantages such as easy operation, high sensitivity, no need for expensive instruments, and good detection results.

In this comprehensive experiment, after adding gold nanoparticles and Hg^{2+} to the solution of Rhodamine B (RhB), the color of RhB solution can be observed to change from red to colorless, accompanied by the change of fluorescence from orange to colorless; combined with the measurement of UV·Vis and fluorescence spectrometer and data analysis of related test results, students can learn the calculation method of detection limit. The experiment is suitable for the fourth year undergraduate students of chemistry, materials chemistry and environmental chemistry to perform comprehensive analytical chemistry experiments.

2. Experimental purpose

(1) Learn the preparation method of Au NPs and understand the concept of gold amalgamation.

(2) To master the basic operating procedures of fluorescence spectroscopy and UV·Vis spectrometer and the corresponding graphical analysis.

(3) Learn how to detect Hg^{2+} by nanoprobe.

(4) master the calculation of the detection limit.

(5) To study hot issues at the forefront of science and expand students' knowledge.

3. Reagents and instruments

3.1. Reagents

Rhodamine B(RhB, 99%), sodium borohydride($NaBH_4$, 98%), chloroauric acid($HAuCl_4·2H_2O$, 99.5%), sodium citrate(99%), concentrated hydrochloric acid(HCl, 36%), concentrated nitric acid(HNO_3, 98%), $Hg(NO_3)_2·H_2O$(98%), $Cu(NO_3)_2·6H_2O$(98%), $Ni(NO_3)_2·6H_2O$(98%), $NaNO_3$(98%), KNO_3(98%), $Ca(NO_3)·4H_2O$(98%), $Co(NO_3)_2·6H_2O$(98%), $Al(NO_3)_3·H_2O$(99.99%), $Zn(NO_3)_2·6H_2O$(98%), $Cd(NO_3)_2·4H_2O$(98%), $Fe(NO_3)_2·9H_2O$ (98%), $Ba(NO_3)_2$ (98%), $Fe(NO_3)_3·9H_2O$ (98%), $Mg(NO_3)_2·6H_2O$ (98%), $Mn(NO_3)_2·4H_2O$ (98%), $Cr(NO_3)_3·9H_2O$ (98%) were purchased from Bailingway Reagent Company. Yellow River water was obtained from Zhongshan Bridge section of Xiguan, Lanzhou, tap water was obtained from this laboratory, and deionized water was prepared by Milli·Q ultrapure water purification device.

3.2. Experimental apparatus

Electronic analytical balance, magnetic heating stirrer, round bottom flask, spherical condenser, magnet, test tube, transmission electron microscope (TEM, alos F200S, FEI, USA), inductively coupled plasma atomic emission spectrometry (ICP·MS, iCAP Qc, Thermo Fisher Instruments, USA), photoelectron spectroscopy (XPS, AXIS UltraDLD, UK Kratos), UV·Vis spectrometer (Cary5000 Agilent Technologies (China) Co., Ltd.), wide·angle X·ray diffractometer (AXS D8Advance, Bruker Instruments, USA), fluorescence spectrometer (RF·5301, Shimadzu (Shanghai) Experimental Equipment Company).

3.3. Calculation formula

The limit of detection (LOD) of this probe system for Hg^{2+} was calculated based on the experimental data of fluorescence titration and UV titration of RhB. The formula is: $LOD=3\sigma/k$, where σ is the standard deviation calculated by using the data of 10 repeated measurements of RhB fluores-

cence spectra; *k* is the slope of the fluorescence titration curve.

4. Experimental steps

4.1. Synthesis of gold nanoparticles

In a 100 mL round-bottomed flask, add 50 mL of HAuCl4 aqueous solution (1 mmol·L^{-1}), and set a spherical condenser on it. Under rapid stirring and refluxing, 5 mL of sodium citrate aqueous solution (38.8 mmol·L^{-1}) was rapidly injected with a syringe, and the heating was continued for 10 min. During this process, the color of the solution will gradually change from light yellow to purple. After 10min, the heating device was removed, and stirring was continued until cooling No.9doi:10.3866/PKU.DXHX201909003105 to room temperature, the product was collected in a glass bottle and placed in a 4°C refrigerator for later use.

4.2. Formulation of mercury and other ions

Using $Hg(NO_3)_2·H_2O$, $Cu(NO_3)_2·6H_2O$, $Ni(NO_3)_2·6H_2O$, $NaNO_3$, KNO_3, $Ca(NO_3)·4H_2O$, $Co(NO_3)_2·6H_2O$, $Al(NO_3)_3·H_2O$, $Zn(NO_3)_2·6H_2O$, $Cd(NO_3)_2·4H_2O$, $Fe(NO_3)_2$ ·$9H_2O$, $Ba(NO_3)_2$, $Fe(NO_3)_3·9H_2O$, $Mg(NO_3)_2·6H_2O$, $Mn(NO_3)_2·4H_2O$, $Cr(NO_3)_3·9H_2O$ solids, the corresponding ionic concentration of 10^{-5} mmol·L^{-1} stock solution was prepared.

4.3. Screening of optimal experimental conditions

5 μL of gold nanoparticle dispersion with a concentration of 0.4 nmol·L^{-1} (measured by ICP·MS) was added to 2 mL of mercury ion solution with different pH of 10^{-7} mmol·L^{-1}, and mixed well. After acting at room temperature for 5 min, 20 μL of aqueous rhodamine B solution with a concentration of 1 μmol·L^{-1} and 20 μL of freshly prepared $NaBH_4$ solution with a concentration of 40 μmol·L^{-1} were added to it in turn. The UV·visible absorption spectra of the reaction solution were measured in the wavelength range of 300–700 nm.

5 μL of gold nanoparticle dispersion with a concentration of 0.4 nmol·L^{-1} was added to 2 mL of mercury ion solution with a concentration of 10^{-7} mol·L^{-1} and mixed well. After acting at different temperatures for 5 min, 20 μL of aqueous rhodamine B solution with a concentration of 1 μmol·L^{-1} and 20 μL of freshly prepared $NaBH_4$ solution with a concentration of 40 μmol·L^{-1} were added to them in turn. The UV·Vis absorption spectra of the reaction solution were measured in the wavelength range of 300-700 nm.

4.4. UV and fluorescence titration experiments on Hg^{2+}

5 μL of gold nanoparticle dispersion with a concentration of 0.4 nmol·L^{-1} was added into 2 mL of different concentrations of mercury ion solution and mixed well. After acting at room temperature for 5 min, 20 μL of aqueous rhodamine B solution with a concentration of 1 μmol·L^{-1} and 20 μL of freshly prepared $NaBH_4$ solution with a concentration of 40 μmol·L^{-1} were added to it in turn. The fluorescence emission spectra of the mixture at the excitation wavelength of 550 nm and the UV−Vis absorption spectra in the wavelength range of 300−700 nm were measured at 1 min intervals.

4.5. Detection of Hg^{2+} in actual water samples

5 μL of gold nanoparticle dispersion with a concentration of 0.4 nmol·L^{-1} was added to 2 mL of mercury ion solution with a concentration of 10^{-7} mol·L^{-1} (prepared with tap water and yellow river water, respectively) and mixed well. After acting at room temperature for 5 min, 20 μL of aqueous rhodamine B solution with a concentration of 1 μmol·L^{-1} and 20 μL of freshly prepared $NaBH_4$ solution with a concentration of 40 μmol·L^{-1} were added to it in turn. The UV−Vis absorption spectra of the reaction solution were measured in the wavelength range of 300−700 nm.

5. Results and Discussion

5.1. Characterization of gold nanoparticles and gold amalgam

As shown in Figure 1A, the gold nanoparticles were monodisperse, and the shape was homogeneous, almost spherical, and the particle size was found to be about 13 nm. as shown in Figure 1B, when Hg^{2+} was added to the gold nanoparticles, the shape and size of the gold nanoparticles did not change significantly, but the UV absorption wavelength of the gold nanoparticles shifted slightly to the short wavelength (from 525 nm to 522 nm, Figure 1E). When a small amount of freshly prepared $NaBH_4$ solution continued to be added, the gold nanoparticles only slightly agglomerated (Figure 1C). Figure 1F shows the high·resolution photoelectron spectroscopy (XPS) spectrum of Hg4*f* in the gold amalgam formed after the addition of Hg^{2+} to the gold nanosolution, and it can be seen from the figure that one peak appears at the binding energy of 99.7 and 103.86 eV each, and it is known from the literature [7] that these two peaks should be attributed to Hg4$f_{7/2}$, Hg4$f_{5/2}$ of Hg^0, respectively, indicating that the valence state of mercury in the gold amalgam is zero valence, indicating that Hg^{2+} is reduced to Hg^0 by the citrate on the gold surface under the catalytic effect of gold, forming gold amalgam alloy nanoparticles [8].

5.2. Exploration of the detection mechanism of this experiment

Since the absolute electronegativity of mercury is less than that of gold [9]. The electron transfer from the mercury atom to the adsorbed RhB is much easier than that from the gold atom. When Hg^{2+} is present, gold nanocatalytic reduction of Hg^{2+} by citrate can form gold amalgam, which can catalyze the reduction reaction of RhB with $NaBH_4$ efficiently and rapidly compared with gold nanoparticles alone, resulting in the change of naked·eye red RhB to colorless reduced rhodamine B (rRhB), accompanied by the change of the fluorescence signal of the solution from orange to colorless (Figure 2), while gold nanoparticles alone gold nanoparticles alone did not change the red color of RhB significantly after the same time of action with RhB. That is, only in the presence of mercury ions, gold nanoparticles can catalyze the conversion of RhB into rRhB, using this property can achieve multi·mode detection of mercury ions.

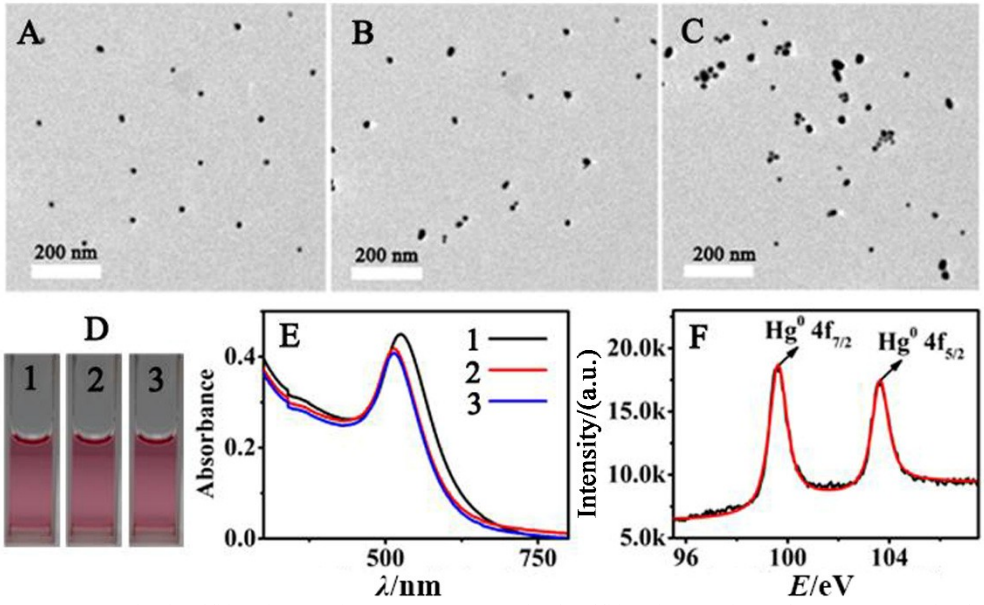

(A) Au NPs TEM; (B) Au NPs TEM after the addition of mercury ions; (C) Au NPs TEM after the addition of mercury ions and $NaBH_4$; (D) (1) color photographs of Au NPs, (2) Au NPs+Hg^{2+}, (3) AuNPs+$NaBH_4$+Hg^{2+}; (E) (1) Au NPs, (2) Au NPs+ Hg^{2+}, (3) UV absorption spectra of AuNPs+$NaBH_4$+Hg^{2+}; (F) XPS high·resolution spectra of gold amalgamated Hg4f

Figure 1. Characterization of gold nanoparticles and gold amalgam

Electronic version is in color

Figure 2. Mercury ion detection mechanism diagram

5.3. Selection of optimal experimental conditions

In order to improve the high sensitivity of mercury ion detection, the experimental conditions (such as temperature and solution pH) need to be optimized before mercury ion detection. Figure 3A shows the changes of absorbance of the solution after adding a certain amount of gold nanoparticles, $NaBH_4$ and a certain amount of mercury ions to a certain concentration of RhB solution at different pHs. It was found that the absorbance of RhB at 550 nm was the smallest when the pH of the solution was close to 7.0. This indicates that RhB was reduced the most when the pH of the solution was 7.0, which means that the catalytic activity of the gold amalgam formed under this pH condition was the highest. Therefore, 7.0 was chosen as the best pH for the assay. In order to evaluate the effect of solution temperature on the catalytic reaction performance, six sets of reaction solutions with different temperatures (15, 20, 25, 30, 45 and 60°C) were selected in the presence of a certain concentration of RhB solution, a certain amount of gold nanoparticles and a certain concentration of mercury ions (Figure 3B). It was found that the absorbance of RhB was the smallest when the temperature of the solution was close to 25°C, which indicated that the amount of RhB was reduced the most at this temperature, indicating that the catalytic activity of gold amalgam was the highest at this temperature, therefore, we chose 25°C as the best reaction temperature for this reaction.

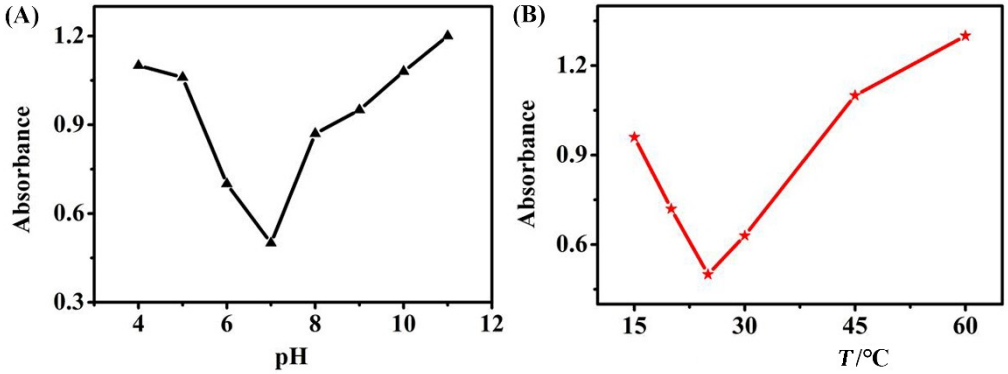

(A) Changes of absorbance of the detection solution under different pH conditions; (B) Changes of absorbance of the detection solution under different temperatures

Figure 3. Screening of optimal experimental conditions

5.4. Selectivity and competition experiments of the detection system for Hg^{2+}

In order to evaluate the selectivity of the detection system for Hg^{2+}, we first selected 17 common ions (Li^+, Na^+, K^+, Cr^{3+}, Cd^{2+}, Cu^{2+}, Zn^{2+}, Ca^{2+}, Co^{2+}, Mn^{2+}, Ba^{2+}, Pb^{2+}, Ni^{2+}, Fe^{2+}, Fe^{3+}, Al^{3+}, Mg^{2+}) in water as interfering ions and investigated The ability of these ions to interfere with the detection system was investigated. First, these interfering ions (100 times the concentration of Hg^{2+}) and Hg^{2+} were added to the detection system. As shown in Figure

4A, we found that the absorbance of the solution changed greatly only in the presence of Hg^{2+}, while the absorbance of the solution remained basically unchanged before and after the reaction of the other interfering ions with the blank sample. Moreover, in the coexistence of interfering ions and Hg^{2+}, Hg^{2+} still significantly enhanced the activity of Au NPs in the catalytic degradation of RhB (Figure 4B). The color of the solution (Figure 4C) and the fluorescence change (Figure 4D) also verified the high selectivity and anti·interference ability of the detection system.

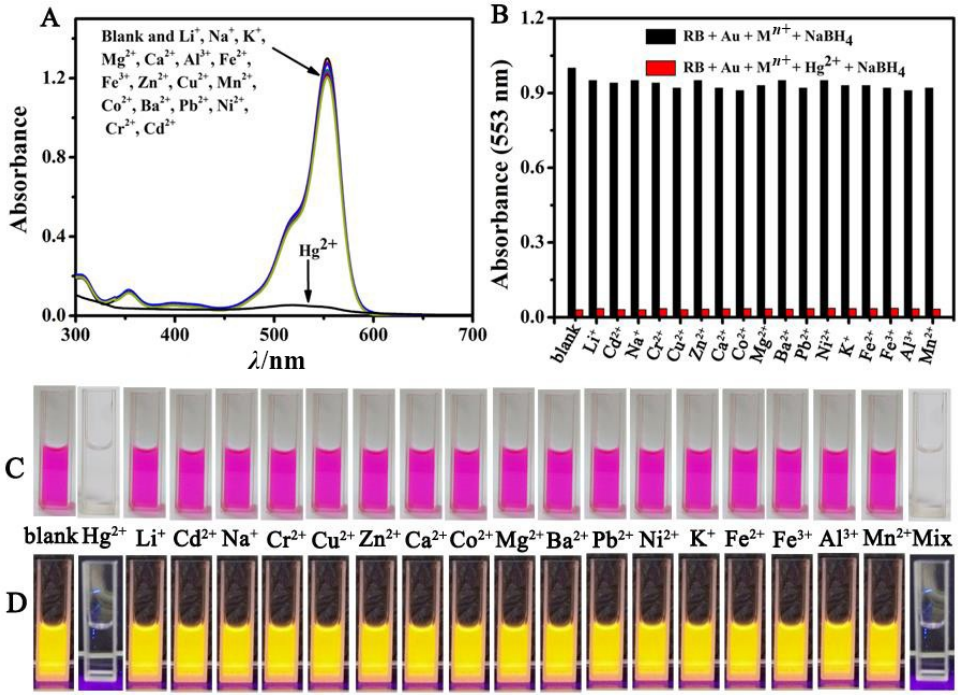

(A) Change of absorbance of solution after adding interfering ions and Hg2+; (B) Change of solution absorbance when Hg2+ coexists with interfering ions; (C) Change of solution color after adding different ions; (D) The solution at 365nm after adding different ions Fluorescent photos under UV light

The electronic version is a color map

Figure 4. Selectivity and competitiveness of detection system for Hg^{2+}

5.5. UV and fluorescence titration experiments of rhodamine B

To evaluate the sensitivity of this detection system, when different concentrations (0, 2, 4, 6, 8, 10, 12, 14, 18, 20, 22, 24, 26 nmol·L^{-1}) of Hg^{2+} were added sequentially to the RhB solution containing Au NPs (10 nmol·L^{-1}), the absorbance of the solution decreased rapidly as the Hg^{2+} concentration gradually increased, the absorbance of the solution decreased rapidly, and the color of the solution also gradually became lighter (Figure 5A). As shown in Figure 5B, the linear range of UV titration was 1−750 nmol·L^{-1}, and we selected a section of the titration curve within the linear range with the linear correlation R^2=0.9983. The limit of detection was calculated from the equation LOD=3σ/k, which was 2.54 nmol·L^{-1}. ·As shown in Figure 5C, with the gradual increase of Hg^{2+} concentration, the fluorescence intensity of the solution gradually decreased, and the fluorescence of the solution also gradually became darker. As shown in Figure 5D, the fluorescence titration curve of Hg^{2+} was plotted from the fluorescence titration experimental data, and its linear range was 1·800 nmol·L^{-1}. We selected a section of the titration curve within the linear range, and its linear correlation R^2=0.9977, and the limit of detection was calculated by the formula LOD=3σ/k 1.16 nmol·L^{-1}.

5.6. Detection of Hg^{2+} in actual water samples

In order to evaluate the ability of this colorimetric and fluorescence dual·signal detection system to detect Hg^{2+} in real water samples, we selected yellow river water, tap water and deionized water to

prepare Hg^{2+} solutions to evaluate the differences of the detection system for Hg^{2+} in different water samples. As shown in Figure 6, when different concentrations of Hg^{2+} were added to tap water, yellow river water and deionized water, the absorbance of the solutions decreased gradually with the increase of Hg^{2+} concentration, and the absorbance values of RhB in the three water samples decreased with the concentration of Hg^{2+} by about the same magnitude without any obvious difference. The linear relationship between fluorescence intensity and Hg^{2+} concentration showed that the detection system was consistent with the results of deionized water detection under laboratory conditions, indicating that the detection system has strong anti·interference ability.

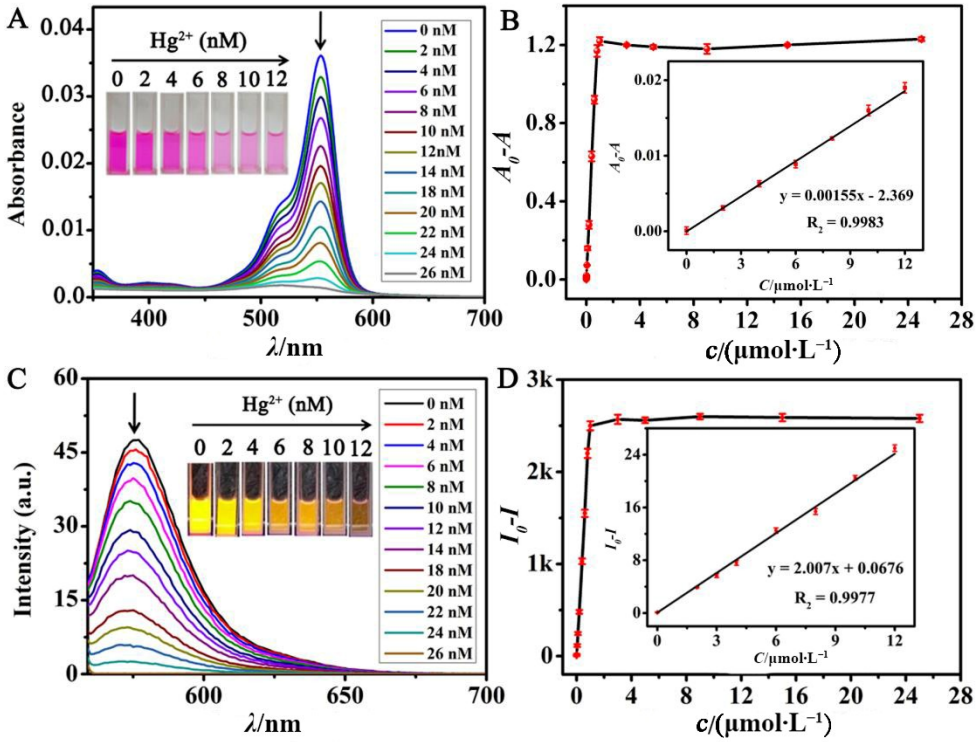

(A) The change of the absorbance of the solution caused by the addition of Hg^{2+}, the inset is the color photo of the corresponding solution; (B) The change curve of A_0–A with the concentration of Hg^{2+}, the inset is its optimized linear range; (C) The addition of Hg^{2+} makes the solution fluorescence intensity (*E*x=550nm, *Slit*: 3nm/3nm), the inset is the fluorescence photo of the corresponding solution; (D) The curve of I_0–I with Hg^{2+} concentration, the inset is its optimized linear range

The electronic version is a color map

Figure 5. UV and fluorescence titration of Hg^{2+} by detection system

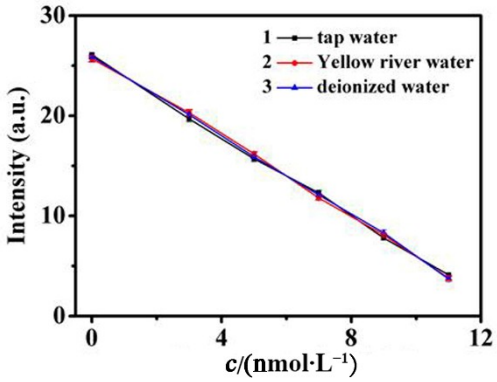

Figure 6. Trend of absorbance of solutions in different water samples with the concentration of Hg^{2+} in the solution

6. Teaching organization and operation methods and teaching methods

The experiment is designed to be up·to·date and open·ended. The lab is 18 hours long, and students are required to conduct literature research prior to the lab. In the first week of 6 hours, students spend 2 hours reporting background knowledge on environmental pollution and the preparation and detection of nanomaterials. This is followed by 4

hours on the preparation of nanomaterials and cross·sectional electron microscopic characterization. The second week is devoted to 6 hours of analytical titrations with UV-Vis and fluorescence spectroscopy for the detection of mercury ions and cross·over to electron microscopic characterization. In the third week, XRD and XPS characterization are crossed over and a brief summary is given. During the teaching process, students will be guided by heuristic teaching method to think deeply and cultivate their sense of innovation. Interested students can join the faculty's related project group to explore the synthesis of related nanoprobes with detection functions for other ions and conduct research on the corresponding ion detection work.

7. Concluding remarks

The experiment follows the current research frontiers and hot spots in the field of scientific research, and meets the requirements of the comprehensive experimental teaching reform of analytical chemistry. The experiment is very close to the students' real life and can easily stimulate their interest. Students will have a certain understanding of the sources of environmental pollutants by reviewing relevant literature, and will be guided to design and synthesize nanoprobes that can be used for the detection of other ions. On the basis of this, the students will be able to develop their horizons, gradually cultivate their innovative ability to ask questions and practice, and cultivate their scientific research ability to design experiments and analyze problems with various instruments in the current hot areas of research.

References

1. Jhansi, R.K.; Tahir, A.; Sadia, A.K.; Adria, N.; Perry, C.; Birsen, V.; Marla, W.; Shardae, M.; Britinia, R.; Santanu, B.; et al. Angew.Chem.Int. Ed, 2009, 121, 9848.
2. Yang, X.; Wang, E.K. Anal.Chem.2011, 83(12), 5005.
3. Ma L·N, Liu D·Jun, Wang Z·X. Analytical Chemistry, 2010, 38, 1.
4. Daniel, M.C.; Astruc, D. Chem. Rev. 2004, 104(1), 293.
5. Katz, E.; Willner, I. Angew. Chem. Int. Ed. 2004, 43(45), 6042.
6. Benoit, J.M.; Fitzgerald, W.F. Environ. Res. 1998, 78(2), 118.
7. Wu, G.W.; He, S.B.; Peng, H.P.; Deng, H.H.; Liu, A.L.; Lin, X.H.; Xia, X.H.; Chen, W. Anal.Chem.2014, 86(21), 10955.
8. Chen, Z.B.; Zhang, C.M.; Gao, Q.G.; Wang, G.; Tan, L.L.; Liao, Q. Anal.Chem.2015, 87, 10963.
9. Pearson, R.G. Inorg. Chem. 1988, 27, 734.